# COMPACT SUPERCONDUCTING RF-DIPOLE CAVITY DESIGNS FOR DEFLECTING AND CRABBING APPLICATIONS*

S. U. De Silva[1,2†], J. R. Delayen[1,2], A. Castilla[1,2,3],
[1]Center for Accelerator Science, Old Dominion University, Norfolk, VA 23529, USA.
[2]Thomas Jefferson National Accelerator Facility, Newport News, VA 23606, USA.
[3]Universidad de Guanajuato (DCI-UG), Departamento de Fisica, Leon, Gto. 37150, Mex.

*Abstract*

Over the years the superconducting parallel-bar design has evolved into an rf-dipole cavity with improved properties. The new rf-dipole design is considered for a number of deflecting and crabbing applications. Some of those applications are the 499 MHz rf separator system for the Jefferson Lab 12 GeV upgrade, the 400 MHz crabbing cavity system for the proposed LHC high luminosity upgrade, and the 750 MHz crabbing cavity for the medium energy electron-ion collider in Jefferson Lab. In this paper we present the optimized rf design in terms of rf performance including rf properties, higher order modes (HOM) properties, multipacting, and multipole expansion for the above mentioned applications.

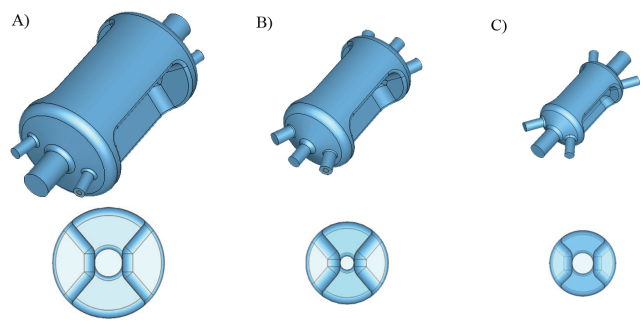


Figure 1: RF-dipole geometries and their corresponding cross sections for the A) 400 MHz, B) 499 MHz and C) 750 MHz designs.

## INTRODUCTION

The rf-dipole geometry is a compact deflecting and crabbing design with very attractive rf properties [1]. The fundamental deflecting and crabbing mode in the rf design is a $TE_{11}$-like mode where the contribution to the deflection is mainly from the transverse electric field. The rf-dipole design has lower balanced surface fields with higher net deflection and higher shunt impedance. The deflecting/crabbing mode is the lowest mode in the rf-dipole design. The rf-dipole cavity prototypes of 400 MHz, 499 MHz and 750 MHz shown in Fig. 1 have been designed and built. The 400 MHz geometry has been tested, and similar tests are under schedule for the other two geometries.

In the rf-dipole geometry, the properties depend on a few design parameters. The frequency is dependent on the outer dimensions, and the ratios of peak surface fields to the transverse electric field are minimized by changing the height and angle of the trapezoidal-shaped loading elements [2, 3]. The rf properties of the three designs are shown in Table 1. As the ratio of the beam aperture diameter to the half wavelength [$d/(\lambda/2)$] increases, the transverse shunt impedance [$R_T R_S$] reduces, and the peak surface field ratio increases.

Table 1: Properties of rf-dipole structures

| Parameter | 400 MHz | 499 MHz | 750 MHz | Units |
|---|---|---|---|---|
| $\lambda/2$ of $\pi$ mode | 374.7 | 300.4 | 200.0 | mm |
| Cavity length | 527.2 | 440.0 | 341.2 | mm |
| Cavity radius | 169.9 | 121.1 | 93.7 | mm |
| Bars width | 80.0 | 50.0 | 63.0 | mm |
| Bars length | 350.3 | 260.0 | 200.0 | mm |
| Bars angle | 50 | 50 | 45 | deg |
| Aperture diameter -$d$ | 84.0 | 40.0 | 60.0 | mm |
| Deflecting voltage -$V_T^*$ | 0.375 | 0.300 | 0.200 | MV |
| Peak electric field -$E_P^*$ | 4.02 | 2.86 | 4.45 | MV/m |
| Peak magnetic field -$B_P^*$ | 7.06 | 4.38 | 9.31 | mT |
| $B_P^*/E_P^*$ | 1.76 | 1.53 | 2.09 | $\frac{\text{mT}}{\text{MV/m}}$ |
| Energy content -$U^*$ | 0.195 | 0.029 | 0.068 | J |
| Geometrical factor | 140.9 | 105.9 | 131.4 | Ω |
| $[R/Q]_T$ | 287.0 | 982.5 | 124.2 | Ω |
| $R_T R_S$ | 4.04 | 10.00 | 1.65 | $\times10^4\Omega^2$ |

At $E_T^*$= 1 MV/m

## HIGHER ORDER MODE PROPERTIES

The HOM spectra for the three geometries are shown in Fig. 2. The fundamental deflecting/crabbing mode is the lowest operating mode (there are no lower order modes in the rf-dipole geometry). The next higher order mode is approximately 1.5 times the frequency of the fundamental operating mode, making the HOM extraction fairly easy.

* Authored by Jefferson Science Associates, LLC under U.S. DOE Contract No. DE-AC05-06OR23177. Part of this work was done in collaboration with and supported by Niowave Inc. under the DOE STTR program. Research also supported by EU FP7 HiLumi LHC - Grant Agreement 284404

† sdesilva@jlab.org





ISBN 978-3-95450-122-9

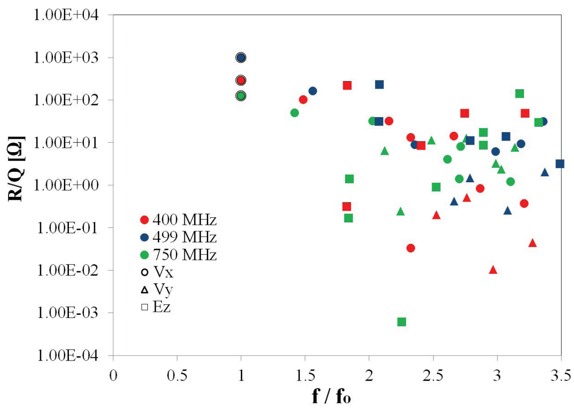


Figure 2: HOM spectra for the three rf-dipole designs. The frequency ($f$) for each mode has been normalized to the corresponding operating frequency ($f_0$).

## MULTIPACTING ANALYSIS

An impediment to maintaining the operation gradients and avoiding thermal breakdown in superconducting cavities is the presence of multipacting. We realized multipacting studies for the three rf-dipole cavities using the SLAC's TRACK3P code from the ACE3P suite. Having found that at the desired operating voltages (3.4/5.0 MV at 400 MHz, 3.0/5.6 MV at 499 MHz and 2.0/8.0 MV at 750 MHz) the rf-dipole does not show critical multipacting levels for the three geometries analyzed in this paper, we will show in the rf-testing section experimental results that suport this statement.

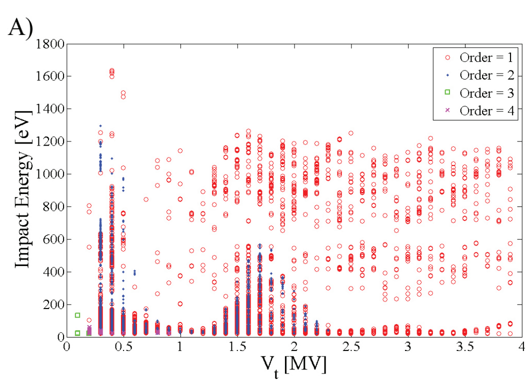


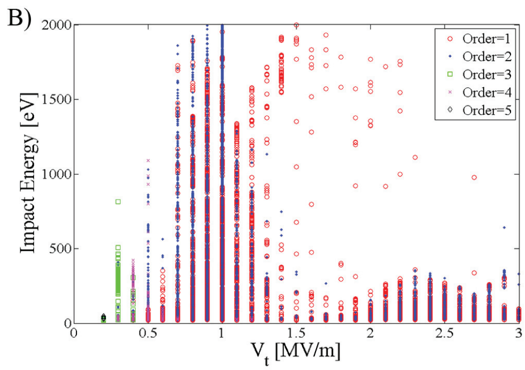


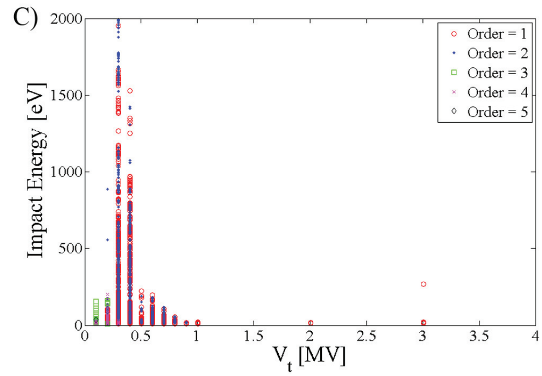


Figure 3: Impact energy for resonant particles as a function of the transverse voltage for the rf-dipole designs A) 400 MHz, B) 499 MHz and C) 750 MHz.

## MULTIPOLE FIELD ANALYSIS

In the rf-dipole design, the field varies across the beam aperture off the beam axis generating a non-uniform transverse deflection. The field variation in $x$ and $y$ directions are shown in Fig. 4 for all the rf-dipole designs mentioned in Fig. 1.

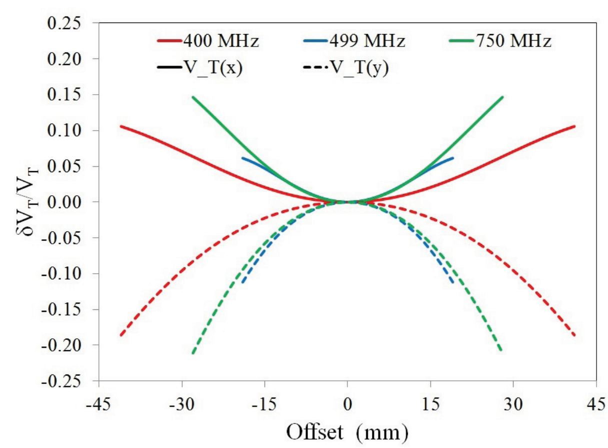


Figure 4: Normalized transverse voltage in $x$ and $y$ directions for desings A), B) and C) from Fig. 1 respectively.

The non-uniform transverse fields can generate higher orders of transverse momentum apart from the first order transverse momentum that corresponds to the deflecting or crabbing voltage [4]. These higher order transverse multipole components may lead to perturbations in the beam and can be reduced either by increasing the bar height or curving the bars around the beam aperture area. The higher order multipole components of the fundamental deflecting/crabbing mode for the three rf-dipole designs in Fig. 1 are shown in Table 2. After inspecting the field profiles the $b_n$ for $n = 0, 2, 4, 6...$ were determined neglegible. All the higher order multipole components are normalized to a transverse voltage ($V_t$) of 1.0 MV.

Table 2: Multipole components for the rf-dipole cavity designs shown in Fig. 1

| | 400 MHz | 499 MHz | 750 MHz | Units |
|---|---|---|---|---|
| $V_T$ | 1.0 | 1.0 | 1.0 | MV |
| $b_1$ | 3.3 | 3.3 | 3.3 | mTm |
| $b_2$ | 0.0 | 0.0 | 0.0 | mT |
| $b_3$ | 3.00 | 8.30 | 1.81 | $\times 10^2$ mT/m |
| $b_4$ | 0.0 | 0.0 | 0.0 | mT/m$^2$ |
| $b_5$ | -0.46 | -5.8 | -5.2 | $\times 10^5$ mT/m$^3$ |

## RF TESTING

The 400 MHz cylindrical rf-dipole design has been successfully tested at the cryogenic temperatures of 4.2 K and 2.0 K at the vertical test assembly at Jefferson Lab. The cavity was fabricated by Niowave Inc. with 3 mm thick Nb sheets of RRR 353-405 [5].

### *Surface Treatment*

The surface treatment process [6] included the initial surface etching with bulk removal of 150 $\mu$m using the standard BCP acid mixture, followed by a heat treatment for 10 hours at 600 C. After the heat treatment the cavity was further etched for a light removal of 10 $\mu$m. Then the cavity was high pressure rinsed in 3 passes. Due to a contamination with glycol in the acid mixture the etch rate was reduced from 2.7-2.8 $\mu$m/min to 1.8 $\mu$m/min that resulted in a total average removal of 85 $\mu$m in the bulk BCP process. Finally the cavity was assembled at the class 10 clean room.

### *RF Test Results*

The cavity underwent a test at 4.2 K and two tests at 2.0 K. In the first 2.0 K test a multipacting resonant condition was observed at low fields and was easily processed by increasing the rf power. No further multipacting conditions were observed during the remaining of the first test or on the following 4.2 and 2.0 K tests. The measured surface resistance of the cavity was 34 n$\Omega$ during the cool down process from 4.2 K to 2.0 K.

The intrinsic quality factor ($Q_0$) as a function of transverse electric field ($E_T$), transverse voltage ($V_T$), peak surface electric field ($E_P$), and peak surface magnetic field ($B_P$) for both 2.0 and 4.2 K tests are shown in Fig 5. The 4.2 K $Q$ curve has a higher slope which is a norm at lower frequency cavities. The cavity was dissipating 155 W at 11.6 MV/m and was limited by the rf power. The test achieved peak surface electric and magnetic fields of 47 MV/m and 82 mT. The 4.2 K rf test achieved a transverse voltage of 4.4 MV exceeding the design requirement of 3.4 MV. The 2.0 K rf test has a uniform $Q_0$ variation compared to that of 4.2 K rf test. The cavity quenched at 18.6 MV/m and achieved a transverse voltage of 7.0 MV and peak surface electric and magnetic fields of 75 MV/m and 131 mT. The 2.0 K rf test exceeded the required transverse voltage of 3.4 MV and can reasonably achieve a transverse voltage of 5.0 MV per cavity.

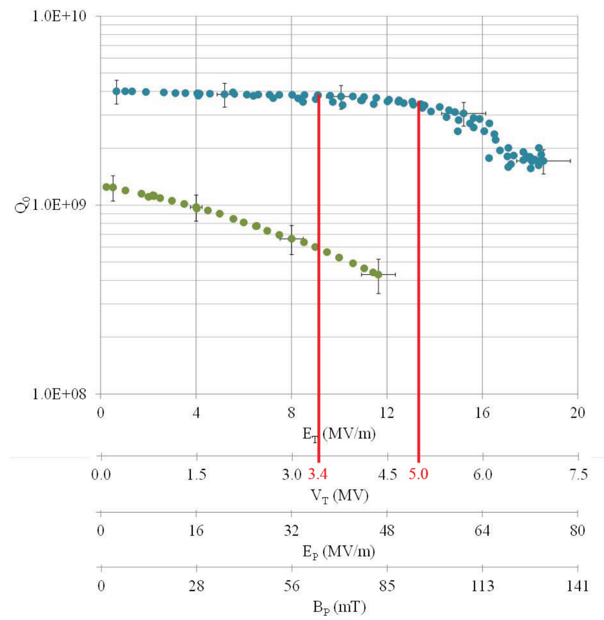


Figure 5: $Q$-curves for the 400 MHz rf-dipole at 4 K (green) and 2 K (blue) as a function of the transverse gradient, transverse voltage and peak values of the fields.

## CONCLUSIONS

An extensive study on the properties of the rf-dipole design have been presented for three different geometries. The performance of a proof of principle cavity has been tested for the 400 MHz geometry. The high gradient reached during this test and the virtual abscence of multipacting at the operating gradients show the rf-dipole as an attractive option for many deflecting and crabbing applications. Similar proof of principle cavities have been built for the 499 MHz and 750 MHz geometries, and the corresponding rf-tests are under schedule for this spring.

## REFERENCES

[1] S.U. De Silva and J.R. Delayen, Phys. Rev. ST Accel. Beams 16, 012004 (2013).

[2] J.R. Delayen and S.U. De Silva, in Proceedings of the 15*th* International Conference on RF Superconductivity, Chicago, Illinois, p. 219 (2011).

[3] A. Castilla et.al., in Proceedings of IPAC'12, New Orleans, Louisiana, p. 2447 (2012).

[4] S.U. De Silva and J.R. Delayen, Multipole Field Effects for the Superconducting Parallel-Bar/RF-Dipole Deflecting/Crabbing Cavities, LINAC 2012, Tel-Aviv, Israel, September 2012.

[5] D. Gorelov et.al., in Proceedings of IPAC'12, New Orleans, Louisiana, p. 2411 (2012).

[6] P. Kneisel, Nucl. Instrum. Methods 557, 1 (2006).




ISBN 978-3-95450-122-9